Competing Patterns in a Convective Binary Mixture

Elisha Moses and Victor Steinberg
Department of Nuclear Physics, Weizmann Institute of Science, Rehovot 76 100, Israel
(Received 19 June 1986)

Pattern observations and heat-transport measurements of convection in ethanol-water mixtures at positive values of the separation ratio ψ are presented. Close to onset, the convective flow manifests itself in a stationary square pattern with negligible change in heat transport compared with the conductive state. Far from threshold, convection selects the usual roll structure with a strong change in heat transport. In a crossover region, the competition between square and roll patterns leads to oscillations.

PACS numbers: 47.25.Qv, 47.20.−k

The interaction between heat and mass diffusion in a binary mixture leads to a remarkable variety of nonlinear behavior just near convective threshold. Most of the recent theoretical developments[1] and experimental observations[2] have concentrated on studying novel nonlinear dynamics such as oscillatory convection and multicritical behavior near the convective onset, features which cannot be observed in a simple fluid. However, recent experimental results on heat transport in stationary convection of a normal ^{3}He-^{4}He mixture heated from below have demonstrated that our understanding of nonlinear heat transport due to stationary convection in a binary mixture is still far from complete.[3,4]

In this Letter, we consider Soret-driven convection in ethanol-water mixtures. The Soret effect is a mechanism by which an externally imposed temperature gradient in a mixture establishes a concentration gradient in a mass-conserving system. A measure of the coupling between temperature and concentration variations is the separation ratio ψ. It is an externally controlled parameter and can be varied by changing the mean temperature and concentration of the sample. It is the sign and value of ψ that determine if the convective state is oscillatory or stationary.[5] At positive ψ, both the temperature gradient and concentration gradient destabilize the system. As a function of the temperature difference across the cell—the second externally controlled parameter—one or another mechanism dominates the flow. Close to convective onset, the motion is dominated by the solute gradient, especially for large positive ψ,[5] and we define this as the Soret regime. The critical temperature difference for the convective onset in a binary mixture, ΔT_c, can be reached considerably at $\psi L^{-1} \gg 1$ compared with ΔT_t of the convective onset (defined as the usual Rayleigh regime) in a simple fluid with the same thermophysical properties as a binary fluid mixture. Here $L = D/\kappa$ is the Lewis number, the ratio between mass diffusivity and thermal diffusivity. Thus, in the case of stationary convection in a binary mixture there are two driving parameters which can be controlled externally, and two regimes of convection exist, each of which can be observed in a different region of the Rayleigh number for fixed value of ψ. When the critical temperature difference for both regimes is very different, the two regimes can be isolated unambiguously.

The intriguing feature of the two regimes is the striking difference in nonlinear behavior, both in heat transport and in pattern and wave number selection, part of which has been predicted by theory.[1,5] In heat transport (measured by the Nusselt number), it manifests itself in very different values of the initial slope S of the Nusselt number versus ΔT for the two regimes. The heat transport for the Soret regime is predicted to be dramatically suppressed.[1a] For larger ΔT, when the system becomes unstable to the Rayleigh mode, S increases dramatically and approaches values of order unity, close to that of convection in a pure fluid.[3]

Boundary conditions for temperature and concentration realizable in the experiment lead to different wave numbers and stable planforms selected. It was realized already in early studies that with impermeable boundary conditions for concentration, linear stability analysis gives at large enough positive ψ a critical Rayleigh number $R_c = 720$ and critical wave number $k_c = 0$.[5a] This cellular structure with great horizontal extent is similar to what has been predicted earlier in the case of the Rayleigh-Bénard convection in a simple fluid with insulating boundaries. We suggest that this analogy should be carried into the nonlinear regime as well, where recent calculations show that the preferred pattern is not a parallel roll structure as for perfectly conducting boundaries, but rather a square pattern.[6] A binary mixture provides a convective system whose boundary conditions correspond to those of perfectly insulating boundaries. This is a situation which is impossible to achieve experimentally with boundary conditions on heat transport. Thus, it is anticipated that two different mechanisms of instability in stationary convection will lead to two different wave numbers and to pattern selection with different nonlinear behavior: square pattern with small wave number for the Soret regime and parallel rolls with $k_c = 3.117$ for the Rayleigh regime.

We present here observations of convective flow patterns in containers of various geometries, simul-

taneous heat transport measurements, and light intensity measurements as a function of time and location in the flow in a room-temperature experiment on ethanol-water mixtures with ψ in the range $0.01 \leq \psi \leq 0.1$.[7]

The experiments were done with ethanol-water mixtures with weight concentration in the range 29.6 wt.% and 40 wt.% of ethanol at a temperature of 25 °C. Our experimental apparatus has been described previously.[2b] In the present experiment, we used several cells. Most of the heat transport measurements and part of the pattern observations were done in a rectangular cell 2.96 mm high, 12.0 mm wide, and 36.0 mm long (the aspect ratio is 1:4:12). Pattern competition was observed in a cylindrical cell with $d = 1.8$ mm high and aspect ratio 20, and in square cells with aspect ratio 8.9 and 24. L is close to 0.018 and only changes slightly with concentration and temperature.

The results on heat transport measurements in the rectangular cell for all samples and for the large square cell with 40 wt.% ethanol are presented in Fig. 1. S is estimated to be in the range 0.00–0.02.[3,4] The slope changes dramatically at ΔT close to the threshold of the Rayleigh regime to the value $S \approx 0.74$–0.77, the same value as we observed for water in the same aspect ratio cell.

Figure 2 shows three typical patterns observed in a rectangular container with aspect ratio 1:4:12. The first pattern [Fig. 2(a)] which is close to a square one, was observed in the range where convection is driven by the concentration gradient. The third pattern [Fig. 2(c)] which clearly shows the usual Rayleigh-Bénard convection roll structure was observed in the range of large S corresponding to the Rayleigh regime of convection. The second type of pattern [Fig. 2(b)] reflects the competition between two structures, and this intermediate type of pattern was observed in a crossover region, where S changes. All three types of patterns are stationary, as confirmed by heat-transport and local-light-intensity measurements. We find that the geometry of the rectangular cell puts strict limitations on the competition between mechanisms, and the transition in patterns coincides with the transition in heat transport.

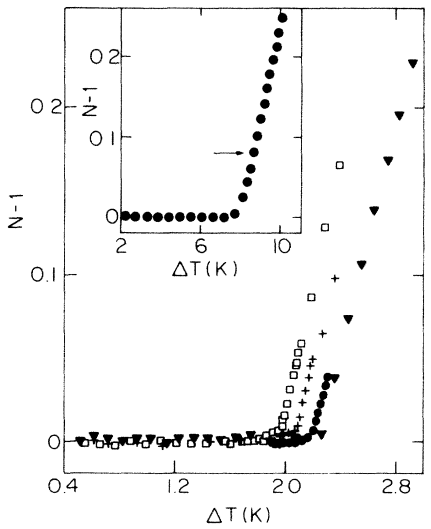

FIG. 1. Convective contribution $N-1$ to heat transport as a function of the temperature difference ΔT across the rectangular cell: (a) squares, 40 wt.%; (b) plusses, 35 wt.%; (c) circles, 31 wt.%; (d) triangles, 29.6 wt.%. In the upper left corner, sample of 40 wt.% in the large square cell. Arrow points at set-in of oscillations.

In order to investigate the nature of the square patterns and their competition with the roll structure in detail, we conducted the same experiment with a mixture of 40 wt.% ethanol in water in containers of various geometries: a cylindrical cell 1.8 mm high and aspect ratio 20, a square cell 1.8 mm high and aspect ratio 24, and a square cell 2.2 mm high and aspect ratio 8.9. In all cells, we followed two different procedures. The first procedure is demonstrated in Fig. 3, for the cylindrical cell. As in the rectangular cell, we increase ΔT above the convective threshold by steps, waiting at each point 20–40 vertical diffusion time depending on the step size. In this case, the square pattern appears first as a disordered stationary structure (reminiscent of a 2D melt) at $\Delta T \simeq 7$ K [see Fig. 3(a)], and then for $\Delta T \simeq 8$ K it changes to an ordered stationary structure which contains several defects and grains [see Fig. 3(b)]. Further increase in ΔT above 8.5 K leads to oscillations in the form of alternatively invading waves, similar to those reported by Le Gal, Pocheau, and Croquette[8] [see Figs. 3(c)–3(f)]. Local-light-intensity measurements show that the amplitude of oscillations increases and the frequency decreases and approaches zero as ΔT is increased. During this period, two per-

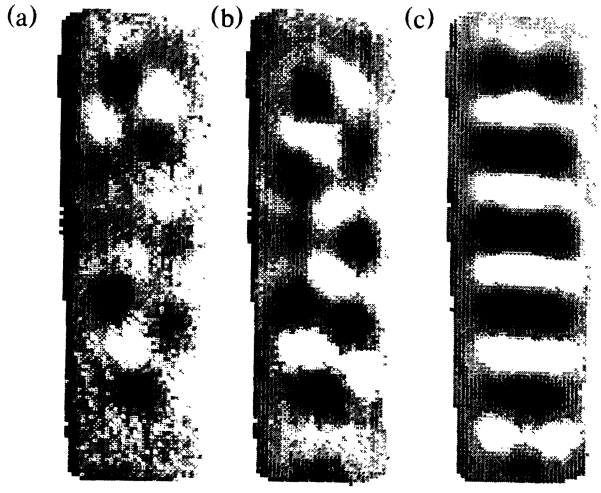

FIG. 2. Flow patterns in rectangular cell for 35 wt.% of ethanol: (a) squarelike pattern at $\Delta T = 1.96$ K; (b) pattern in crossover region at $\Delta T = 2.085$ K; (c) roll pattern at $\Delta T = 2.20$ K.

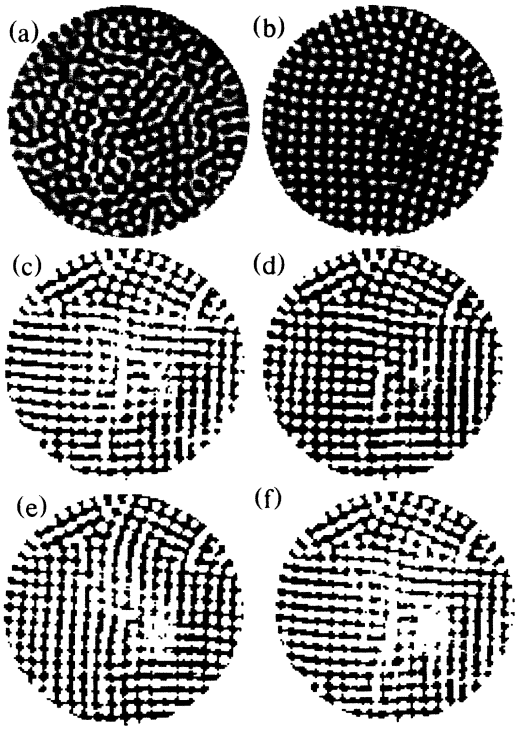

FIG. 3. Shadowgraph pictures of "natural" flow patterns in cylindrical cell with 40 wt.% of ethanol: (a) disordered square pattern at $\Delta T \simeq 8.0$ K; (b) ordered square pattern at $\Delta T \simeq 8.8$ K; (c), (d), (e), (f) pictures of oscillating square patterns at $\Delta T \simeq 9.4$ K. The time sequence for pictures during the cycle is $t = 0$ for (c), $t = 6$ min for (d), $t = 12$ min for (e), and $t = 24$ min for (f).

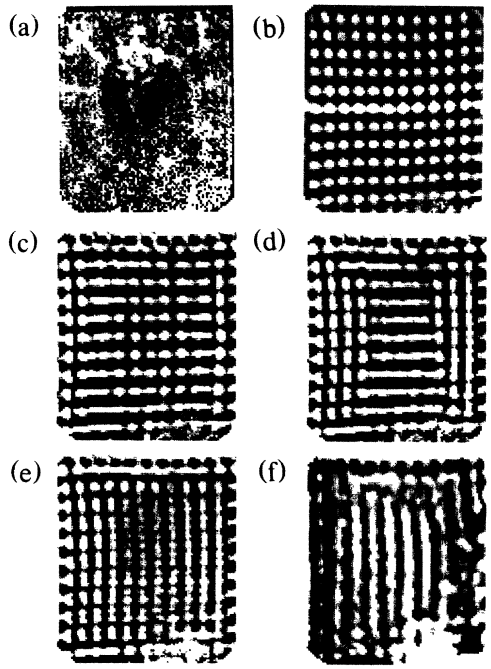

FIG. 4. Flow patterns in square cell of aspect ratio with 40 wt.% of ethanol: (a) large scale flow close to the convective threshold at $\Delta T = 2.312$ K; (b) induced "perfect" square grid at $\Delta T = 8.466$ K; (c), (d), (e) sequential pictures of the oscillating structure at $\Delta T = 9.28$ K (the difference between pictures is 7 min); (f) roll pattern at $\Delta T \simeq 17.9$ K.

pendicular sets of rolls in each of the grains alternatively invade from the boundary to the interior of the cell. Further increase in ΔT leads to roll structure at ΔT on the order of 14 K. This scenario was observed for about the same values of $\Delta T/\Delta T_c$ in the square cells with aspect ratios 8.9 and 24. From these we can conclude that the oscillations observed are an intrinsic property of the pattern competition, rather than topologically induced.

The characteristic size of the square pattern is on the order of the cell height d. This wavelength remains stable against long-wave perturbations, and the square pattern has a tendency to decrease the wavelength. The latter statement follows from the experiment on the small square cell with aspect ratio 8.9 where 9×9 squares were observed. It should be pointed out that the ordered square patterns and the scenario that follows persisted and were observed far above the transition in heat transport to the Rayleigh convective regime. This conrasts with the scenario observed in the rectangular cell where the transition from square to roll structure coincides with the crossover regime in heat transport.

In order to study coherent oscillations of the entire structure, we used the second procedure—induction of "perfect" patterns.[9] Since the ordered structure appears well above the convective threshold ($\Delta T \simeq 8$ K), we were able to get defect-free pattern only in the square cells where a healing process over 24 h assisted in the induction [Fig. 4(b)]. In the big square cell this pattern was stationary up to $\Delta T \simeq 8.6$ K, and then small-amplitude oscillations of the entire structure with a frequency of about 1.1 mHz set in [Figs. 4(c)–4(e)]. The oscillations are initially symmetric and almost sinusoidal. As ΔT increases they become more asymmetrical and relaxational with the amplitude of the preferred roll much larger than that of the other roll [Fig. 5(a)]. Double-frequency regular oscillations were observed also in temperature measurements. Frequency as a function of ΔT is presented in Fig. 5(b). The dependence of frequency on ΔT is of a functional form between linear and logarithmic,[1b,2b] with initial period of oscillations between the vertical and horizontal diffusion time scales.

These squarelike patterns indicate the similarity between convection driven by the concentration gradient with impermeable boundary conditions and Rayleigh-Bénard convection with perfectly insulating boundaries.[6] In the latter case, the nonlinear analysis which determines the domain of existence of a stable square pattern relies on the fact that the critical wave number k_c should be infinitely small[6] (or, at least, on

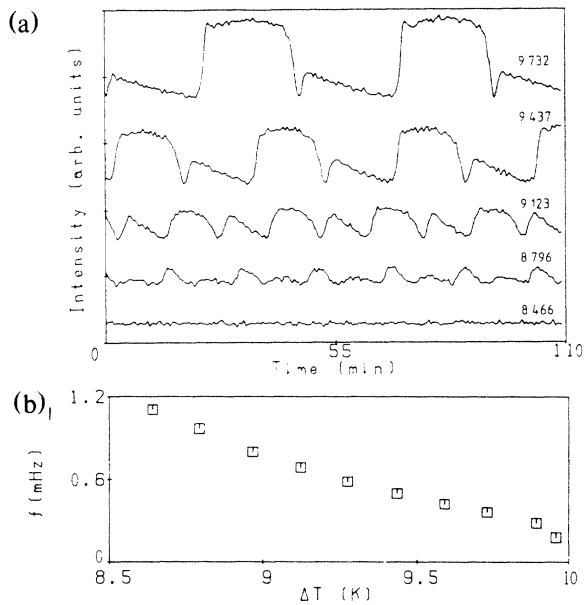

FIG. 5. (a) The light intensity of the shadowgraph at a chosen location in the large square cell with 40 wt.% of ethanol for five different values of temperature difference across the cell ΔT. The numbers given on the figure are ΔT in kelvins. (b) The frequency of light intensity oscillations as a function of temperature difference across the cell.

the order of the inverse aspect ratio). As clearly seen from the patterns, the wavelength for both types of patterns is close to $\lambda_c \simeq 2d$. To investigate this, we conducted a slow scan in ΔT near the convective threshold and observed that already at $\Delta T \simeq 0.44$ K ($\Delta T/\Delta T_c \simeq 1$) and above a large scale structure in the interior of the cell appears, modulated by a spokelike structure induced by the boundaries [see Fig. 4(a)]. This structure is stable and stationary, and exists in a wide temperature range. A new small-scale square pattern (order of d) arises and develops on top of the large-scale structure. This process does not correspond to a prediction of nonlinear analysis that the wavelength decreases as ΔT increases above onset.[6b]

These results shed new light on various known experimental data. Observations of square patterns for moderately conducting boundaries came as a surprise,[8] since convection in water with similar conditions for heat conductance shows no square patterns for $\Delta T/\Delta T_c$ as small as 1.01.[10] The first suggestion came from Le Gal, Pocheau, and Croquette[11]: Oil is a multicomponent fluid. Its Soret coefficient is unknown and, probably, very small. Second, the authors of Ref. 8 noted that the bifurcation between the conductive and the convective states seems imperfect. However, on the basis of our experience with binary mixtures, we can immediately recognize in Fig. 2 of Ref. 8 a small slope between values -0.05 and 0 of ϵ, as in Soret convection. Thus, we conjecture that the phenomena reported in Ref. 8 have the same origin as those reported in this Letter.

In conclusion, we have presented experimental evidence of a system in which domination by different mechanisms leads to novel pattern selection and nonlinear behavior, and competition between these mechanisms leads to intricate oscillations in a crossover region.

This work was supported by the U.S.–Israel Binational Science Foundation Grant No. 8400256 and the Minerva Foundation (Munich, Germany). One of us (V.S.) acknowledges the support of an M.M. Boukstein Career Development Chair.

[1a]H. Brand and V. Steinberg, Phys. Lett. **93A**, 333 (1983); H. Brand, P. C. Hohenberg, and V. Steinberg, Phys. Rev. A **27**, 591 (1983), and **30**, 2584 (1984); E. Knobloch and M. R. E. Proctor, J. Fluid Mech. **108**, 291 (1981); P. N. Coullet and E. A. Spiegel, SIAM J. Appl. Math. **43**, 776 (1983).

[1b]E. Knobloch, to be published.

[2a]I. Rehberg and G. Ahlers, Phys. Rev. Lett. **55**, 500 (1985); R. W. Walden, P. Kolodner, A. Passner, and C. M. Surko, Phys. Rev. Lett. **55**, 496 (1985).

[2b]E. Moses and V. Steinberg, Phys. Rev. A **34**, 693 (1986).

[3]G. Ahlers and I. Rehberg, Phys. Rev. Lett. **56**, 1373 (1986).

[4]H. Gao and R. P. Behringer, Phys. Rev. A **34**, 697 (1986).

[5a]D. T. J. Hurle and F. Jakeman, J. Fluid Mech. **47**, 667 (1971).

[5b]V. Steinberg, J. Appl. Math. Mech. (USSR) **35**, 335 (1971); D. Gutkowicz-Kruzin, M. A. Collins, and F. Ross, Phys. Fluids **22**, 1443,1457 (1979).

[6a]F. H. Busse and N. Riahi, J. Fluid Mech. **96**, 243 (1980); M. R. E. Proctor, J. Fluid Mech. **113**, 469 (1981); V. L. Gertsberg and G. I. Sivashinsky, Prog. Theor. Phys. **66**, 1219 (1981).

[6b]D. R. Jenkins and M. R. E. Proctor, J. Fluid Mech. **139**, 461 (1984).

[7]Our estimates of ψ are based, first of all, on available data on properties of ethanol-water mixtures, which our experience shows are reliable to within 50% near $\psi = 0$. Using linear analysis for $\Delta T_c(\psi)$ and the ΔT at which the first observable pattern appears, we find for 40 wt.% ethanol in the large square container $\psi = 0.1$, in excellent agreement with estimates from available data. For 29.6 wt.% ethanol, this gives a lower limit on $\psi \geq 0.007$.

[8]P. Le Gal, A. Pocheau, and V. Croquette, Phys. Rev. Lett. **54**, 2501 (1985).

[9]M. M. Chen and J. A. Whitehead, Jr., J. Fluid Mech. **31**, 1 (1968).

[10]V. Steinberg, G. Ahlers, and D. S. Cannell, Phys. Scr. **32**, 534 (1985); E. Moses and V. Steinberg, unpublished.

[11]P. Le Gal, A. Pocheau, and V. Croquette, private communication.

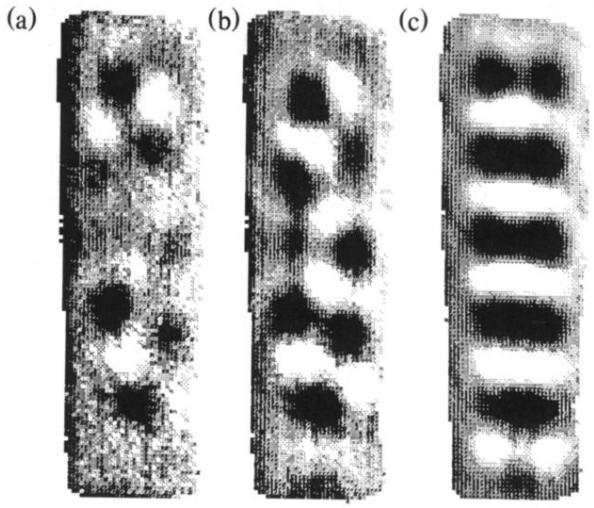

FIG. 2. Flow patterns in rectangular cell for 35 wt.% of ethanol: (a) squarelike pattern at $\Delta T = 1.96$ K; (b) pattern in crossover region at $\Delta T = 2.085$ K; (c) roll pattern at $\Delta T = 2.20$ K.

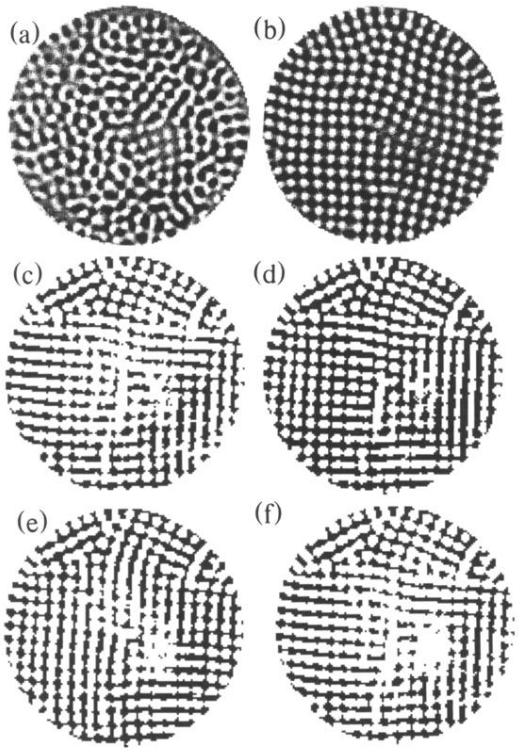

FIG. 3. Shadowgraph pictures of "natural" flow patterns in cylindrical cell with 40 wt.% of ethanol: (a) disordered square pattern at $\Delta T \simeq 8.0$ K; (b) ordered square pattern at $\Delta T \simeq 8.8$ K; (c), (d), (e), (f) pictures of oscillating square patterns at $\Delta T \simeq 9.4$ K. The time sequence for pictures during the cycle is $t = 0$ for (c), $t = 6$ min for (d), $t = 12$ min for (e), and $t = 24$ min for (f).

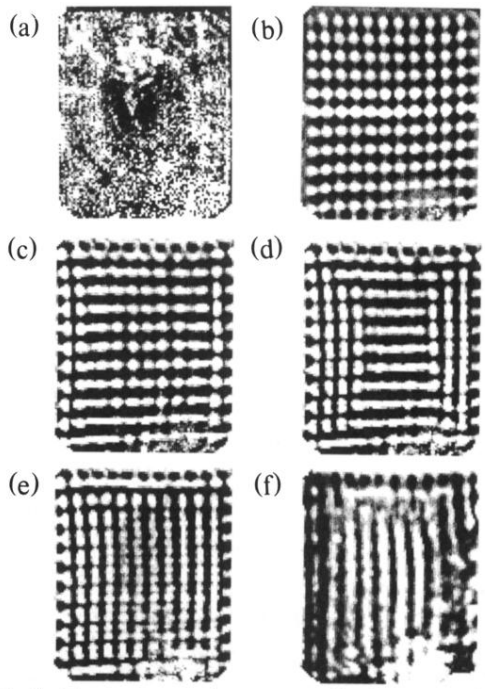

FIG. 4. Flow patterns in square cell of aspect ratio with 40 wt.% of ethanol: (a) large scale flow close to the convective threshold at $\Delta T = 2.312$ K; (b) induced "perfect" square grid at $\Delta T = 8.466$ K; (c), (d), (e) sequential pictures of the oscillating structure at $\Delta T = 9.28$ K (the difference between pictures is 7 min); (f) roll pattern at $\Delta T \simeq 17.9$ K.